ASPARTATE AMINOTRANSFERASE SUBSTRATE SPECIFICITY ALTERATION

Cassandra A. Ricketts

Capstone Advisor: Kathryn Muratore, Ph. D

Capstone Completed Spring 2011

Graduating with University Honors in Biochemistry

Major: Biochemistry, College of Arts and Sciences

ABSTRACT

The purpose of this project is to broaden the specificity of *E. coli* aspartate aminotransferase (eAATase) by mutating it. AATase has narrow specificity, while tyrosine aminotransferase (TATase) is similar to AATase, but has a much broader specificity. Through comparison of the amino acid sequences of TATase and AATase from different organisms, residues predicted to be involved in specificity of aminotransferases are mutated. The specificity of the wild-type eAATase for both aspartate and phenylalanine is confirmed through kinetic determination of k_{cat}/K_m, using a UV-Vis spectrophotometer to measure reaction rates. Sites for mutagenesis based on their predicted involvement in substrate specificity are being selected and will be introduced into the eAATase amino acid sequence. After the mutated enzymes are expressed, each mutant's substrate specificity will be assessed.

INTRODUCTION

The goal of this project is to carry out site-directed mutagenesis in *Escherichia coli* aspartate aminotransferase (eAATase) in order to change its specificity to that of *E. coli* tyrosine aminotransferase (eTATase). Aminotransferases, (also called transaminases), catalyze the transfer of an amino group: the amino group is removed from an amino acid molecule, forming its keto acid, and transferred to a keto acid molecule, converting it to its amino acid form. AATase has a narrow specificity, using aspartate and glutamate, (and their corresponding keto-acids) as substrates (1). Tyrosine aminotransferase is a paralog of AATase: it has a similar amino acid sequence, but a much broader specificity (2). TAT readily uses aspartate, glutamate, tyrosine, and phenylalanine (and their corresponding keto-acids) as its substrates for transamination (1,2).

Figure 1. Aspartate Aminotransferase Homo Dimer [a]

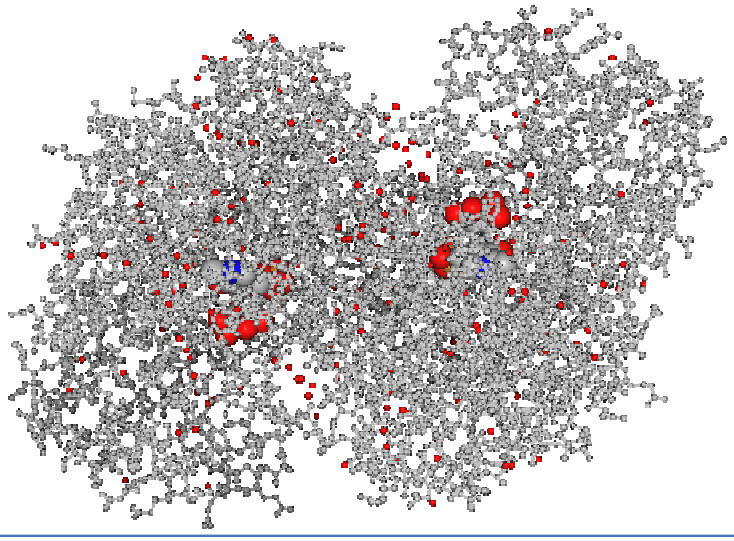

[a] From *reference 5.* Active sites highlighted in red and blue.

Aspartate aminotransferase is a pyridoxal-phosphate- dependent protein: it uses PLP as its cofactor for the transamination (3). AATase exists as a homo dimer *in vivo*, as seen in its structure in Figure 1; and each dimer has an active site for the substrate and the PLP cofactor (4). AATase catalyzes the reversible transfer of an amino group from aspartate to α-ketoglutarate, resulting in the formation

of the amino acid glutamate and the keto acid oxaloacetate as seen in Scheme 1 (1). This reaction has a ping-pong, bi-bi mechanism, a double displacement mechanism in which two substrates are involved (6). AATase is easily able to catalyze the transamination using the polar dicarboxylic acid substrates in Scheme 1, while it is a poor catalyst for the reaction in Scheme 2 with the non-polar aromatic ring of phenylalanine (7). TATase catalyzes the transamination reaction of the many substrates previously listed, but the one currently studied involves the transfer of an amino group from phenylalanine to form phenylpyruvate, as illustrated in Scheme 2 (1). TATase is known to be an excellent catalyst for both the dicarboxylic substrates and the aromatic substrates as seen in Schemes 1 and 2, respectively (8).

Scheme 1: AATase catalyzed reaction[a]

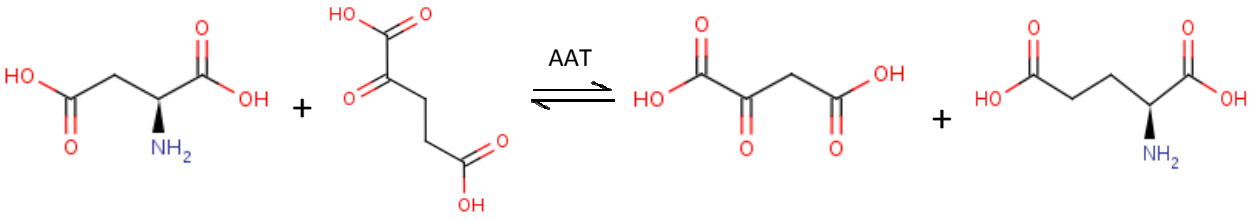

L-aspartate α-ketoglutarate oxaloacetate L-glutamate

[a] From *reference 1.*

Scheme 2: TATase catalyzed reaction[b]

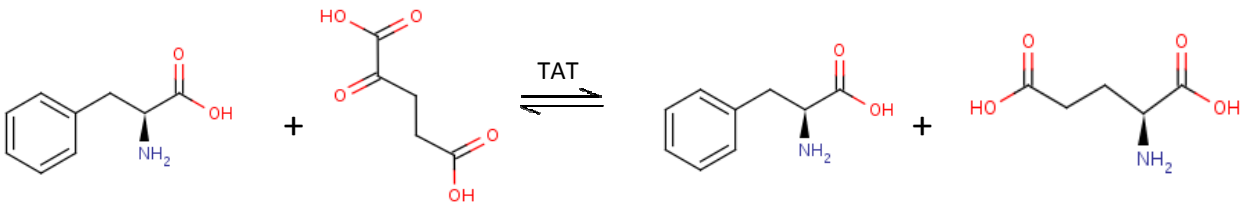

L-phenylalanine α-ketoglutarate phenylpyruvate L- glutamate

[b] From *reference 1.*

Previous studies have worked to redesign the specificity of AATase to that of TATase. Jager, et al. prepared an aspartate aminotransferase mutant V39L and assessed the k_{cat}/K_m values for various substrates (9). The ratio was found to increase for phenylalanine due to lower K_m values (9). Other

researchers performed site-directed mutagenesis of six active site residues: two of which are invariant in all AATase enzymes, but differ in TATase enzymes (10). The other four mutations involved switching of residues to have hydrophobic side chains, in order to redesign the specificity of AATase. This AATase mutant with all six mutations (HEX), was 1000x as reactive with phenylalanine as compared to wild-type eAATase (10). However, HEX was characterized by low dissociation constants and low K_m values for dicarboxylic substrates (11). More investigations of eAATase indicate the role of residue valine 39 of the AATase in the enzyme's specificity (9, 12, 13).

Aspartate aminotransferase and TATase are paralogs, with 72% sequence similarity and 43% sequence identity. However, AATase only has 0.01% of the TATase activities for phenylalanine (in terms of k_{cat}/K_m) (10, 2). Thus, in this project, the amino acid sequences of these two enzymes across different organisms were examined for covariation. Covariation occurs when there are AATase residues which simultaneously differ from residues of TATase throughout many organisms, with the idea that these residues have a possible role in the AATase specificity. Previously in this project, a protein sequence alignment between AATase and TATase was done; then the computer program Patterns (Muratore, unpublished) was used to determine covarying residues. Using the data from Patterns, residues for mutagenesis are being selected based on the distances between the unconserved residues and proximity to the active site. A mutation in residue 39 will be induced along with other covarying residues, because of the suggested role Val 39 has in the specificity in eAATase. The goal of these mutations in AATase is to give aspartate aminotransferase the specificity of TATase.

In this portion of the project, steady-state kinetics of wild-type eAATase were carried out to assess the baseline specificity for aspartate and phenylalanine. Kinetics was carried out using a UV-Vis spectrophotometer, using coupling enzymes malate dehydrogenase and hydroxyisocaproate dehydrogenase for the aspartate and phenylalanine reactions, respectively. Both coupling enzymes catalyze the oxidation of NADH to NAD^+, allowing a loss of NADH to be measured on the

spectrophotometer as a measure of the amount of aspartate/phenylalanine consumed. Using the steady-state kinetic data, k_{cat}/K_m was determined and compared for aspartate and phenylalanine, as a measure of enzyme specificity. After possible mutations involved in specificity of eAATase are induced, the mutant protein will be tested for k_{cat}/K_m for aspartate and phenylalanine, assessing any change in enzyme specificity.

MATERIALS AND METHODS

Steady-State Kinetics of eAATase Using Aspartate. The steady-state kinetics of eAATase using aspartate (Asp), and α-ketoglutarate (αKG) as a cosubstrate, were first carried out using a Shimadzu UV-2550 UV-Vis spectrophotometer. Kinetic assays were performed in 200 mM TAPS buffer (N-Tris(hydroxyl-methyl)methyl-3-aminopropanesulfonic acid), pH 8.0, 100 mM KCl, 10 µM PLP (cofactor pyridoxal phosphate), 150 µM NADH (nicotinamide adenine dinucleotide), and varying concentrations of α-ketoglutarate and aspartate (total volume 1000 µL). Malate dehydrogenase (MDH) was added to the solution (384 U/mL), then the absorbance of the solution was measured for 100 seconds, at 340 nm, where NADH absorbs strongly (14). The background rate was measured with all reagents except aminotransferase. MDH was used as a coupling enzyme because it is involved in the oxidation of NADH to NAD^+, allowing measurement of the change in absorbance per time at 340 nm (1). The concentration of MDH was high enough to ensure that reaction rates measured were independent of the concentration of coupling enzyme. Following the background absorbance measurement, the 1.376 nM eAATase was added, and the change in absorbance was recorded for 100 seconds. The reaction rate was measured for solutions with varying concentrations of both α-ketoglutarate and aspartate: 0.25, 0.50, 1.0, 2.0, and 5.0 mM each. These concentrations created a 25 point kinetic assay grid, and this grid was performed three times.

Using a non-linear least squares fitting function in the data analysis program *Origin,* the data sets were fit according to Equation 1, which is the equation for the ping-pong, bi-bi mechanism (15). Using this fit, the k_{cat} and K_m values were determined for each grid.

$$v = \frac{V_{max}[\text{Asp}][\alpha\text{KG}]}{K_m^{\alpha\text{KG}}[\text{Asp}] + K_m^{\text{Asp}}[\alpha\text{KG}] + [\text{Asp}][\alpha\text{KG}]} \quad (1)$$

Simulation curves were then prepared using the ping-pong, bi-bi equation in *Origin,* plotting velocity of reaction *versus* the concentration of substrate (Michaelis-Menten plot) along with the simulation curve. Then, the data were linearized using the double-reciprocal ping-pong bi-bi simulation curves, using to Equation 2. These simulation curves plotted 1/velocity of reaction *versus* 1/concentration of substrate.

$$1/v = \frac{\boldsymbol{K_m}^{\mathbf{Asp}}\, 1/[\mathrm{Asp}] + \boldsymbol{K_m}^{\boldsymbol{\alpha KG}} 1/[\alpha\mathrm{KG}] + 1}{V_{max}} \qquad (2)$$

Steady-State Kinetics of eAATase Using Phenylalanine. The steady-state kinetic assays were then prepared for the reaction of eAATase with phenylalanine and α-ketoglutarate as the cosubstrate. First, the amount of enzyme required for the k_{cat} and K_m determination was established. Again, a coupling enzyme was used, hydroxyisocaproate dehydrogenase (HicDH), which oxidizes NADH into NAD^+, allowing the measurement of loss of NADH with the spectrophotometer (1). The same method was utilized for the kinetic assays as for the eAATase reaction with aspartate: the reaction ran for 100 seconds, recording absorbances every second. Each kinetic assay was performed in 200 mM TAPS buffer, pH 8.0, 100 mM KCl, 5 µM PLP, 150 µM NADH, 30 mM phenylalanine, and 5 mM α-ketoglutarate. Then, varying amounts and concentrations of HicDH and eAATase were added and the rate was recorded using the spectrophotometer. Enzyme concentration was varied in order to get a rate which showed adequate loss of NADH, and was relatively constant as HicDH concentration was increased, indicating that the rate was unaffected by the concentration of coupling enzyme.

The phenylalanine k_{cat} and K_m determination was carried out using eAATase and varying concentrations of phenylalanine (phe). Each kinetic assay was performed in 200 mM TAPS buffer, pH 8.0, 100 mM KCl, 5 µM PLP, 150 µM NADH, and 5 mM α-ketoglutarate. Varying amounts of

phenylalanine was added to each assay, making solutions of the following concentrations: 48, 24, 12, 6.0, 3.0, 1.5, and 0.70 µM phenylalanine solutions. Then, as previously determined, 846 U/mL HicDH was added to assay, and the background rate was recorded. The 68.75 nM eAATase enzyme was added and each kinetic assay ran for 100 seconds, measuring the reaction rate for each concentration of phenylalanine.

Using the data from the phenylalanine kinetic assays, the Michaelis Menten equation, Equation 3, was used in order to determine the V_{max}/K_m (15).

$$v = \frac{V_{max}[\text{Phe}]}{K_m^{\text{Phe}} + [\text{Phe}]} \qquad (3)$$

In this determination, $[\text{Phe}] << K_m^{\text{Phe}}$, so the [Phe] in the denominator of Equation 3 can be cancelled out, giving Equation 4.

$$v = \frac{V_{max}[\text{Phe}]}{K_m^{\text{Phe}}} \qquad (4)$$

Equation 4 shows the slope of the linear region of the Michaelis Menten plot (velocity *versus* concentrations of substrate) to be equivalent to V_{max}/K_m. Using *Origin,* a linear curve fit was performed on the data, giving the slope and error of the fitting. The linear part of the Michealis Menten plot occurs, as seen here, when at very low concentrations of substrate. Since the K_m is the maximum velocity divided by the concentration of enzyme, the V_{max}/K_m was divided by the concentration of eAATase in order to get the ratio of k_{cat}/K_m.

Selection of Residues for Mutagenesis. Currently, residues predicted to change eAATase specificity are being selected for mutagenesis. Based on the output of the computer program Patterns, residues which showed covariation were sorted into lists, and each list included residue 39. This list of possible residues to mutate will now be used by a PyTrip computer program (Sheftel & Muratore, unpublished) to give an

output of distances between each of the residues. The output with the shorter distances between residues (>10 Å) is opened in PyMOL (DeLano Scientific, 2002) to be visualized in the eAATase structure (PDB entry 1ASM (16)). The AATase cartoon structure from PyMOL is represented in Figure 2. Residues which have shorter distances and a possible role in substrate interactions, may be selected as residues for site-directed mutagenesis.

Figure 2. Aspartate Aminotransferase PyMOL Visualization[a]

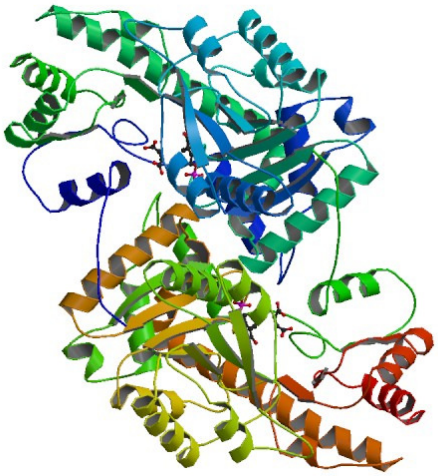

[a]PDB entry 1ASM from reference *16*

RESULTS

Steady-State Kinetics of eAATase Using Aspartate. The calculated reaction rates, μM/s, are given in Table 1 for the eAATase kinetic assays using aspartate. The simulated curves and data were combined in the Michaelis Menten plots and Lineweaver Burk plots, as seen in Figures 3-6 for each grid, illustrating the ping-pong, bi-bi reaction mechanism. Figure 3 shows the Michaelis Menten plots for velocity *versus* the concentration of αKG at each concentration of aspartate. Figure 4 shows the Michaelis Menten plots for aspartate, at each concentration of α-ketoglutarate. The maximum reaction rate that these curves reach has a value of V_{max}, and at half this value, ½ V_{max}, is where the substrate concentration has a value of K_m. Figure 5 shows the reciprocal of velocity *versus* the reciprocal of α-ketoglutarate concentration, at each aspartate concentration. Figure 6 shows the reciprocal of velocity verses the reciprocal of aspartate concentration, at each α-ketoglutarate concentration. For these Lineweaver Burk plots, the x-intercept, is equivalent to $-1/K_m^{App}$ of that substrate. Also, the y-intercept is $1/V_{max}^{App}$ and the slope is equal to K_m/V_{max}.

Table 1. Kinetic Assays Of Varying Concentrations of Aspartate and α –ketoglutarate

Reaction Rates, μM/s:		**[Asp], mM**				
		0.25	**0.50**	**1.0**	**2.0**	**5.0**
[akG], mM	**0.25**	0.0217	0.0280	0.0327	0.0469	0.0525
		0.0310	0.0297	0.0374	0.0344	0.0392
		0.0192	0.0340	0.0306	0.0495	0.0499
	0.5	0.0393	0.0384	0.0497	0.0695	0.0765
		0.0235	0.0381	0.0493	0.0508	0.0657
		0.0231	0.0358	0.0418	0.0579	0.0634
	1.0	0.0296	0.0483	0.0694	0.0898	0.1270
		0.0323	0.0372	0.0651	0.0660	0.0844
		0.0270	0.0400	0.0574	0.0733	0.1022
	2.0	0.0324	0.0467	0.0847	0.0948	0.1430
		0.0335	0.0468	0.0652	0.0875	0.0963
		0.0335	0.0491	0.0593	0.0818	0.1139
	5.0	0.0306	0.0447	0.0766	0.1384	0.1618
		0.0398	0.0724	0.0727	0.0982	0.1554
		0.0292	0.0527	0.0895	0.0921	0.1367

Figure 3. Michaelis Menten Plots of velocity vs. [αKG], at varying concentrations of Asp

a. Grid #1

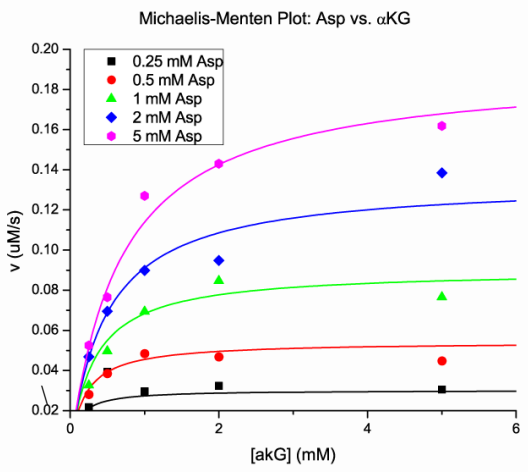

b. Grid #2

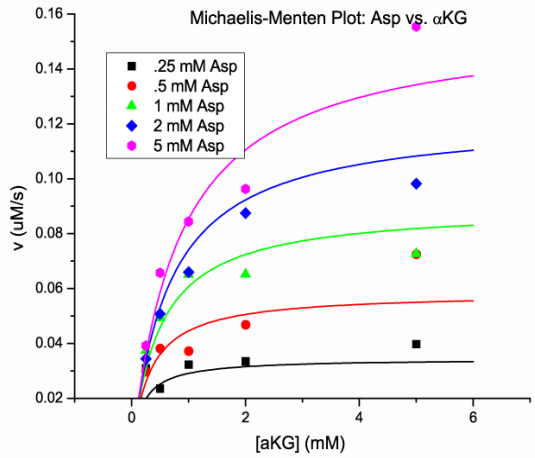

c. Grid #3

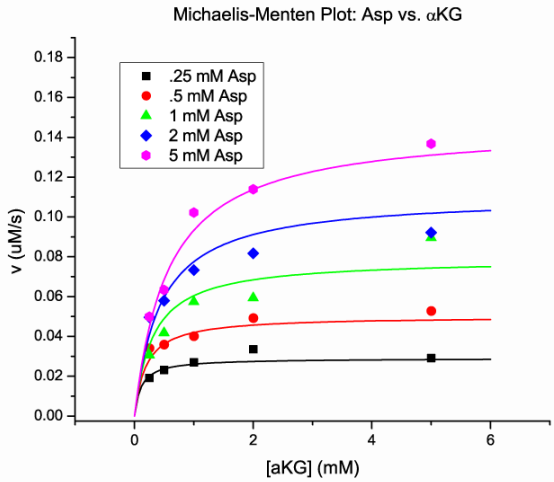

Figure 4. Michaelis Menten Plots of velocity vs. [Asp], at varying concentrations of αKG

a. Grid #1

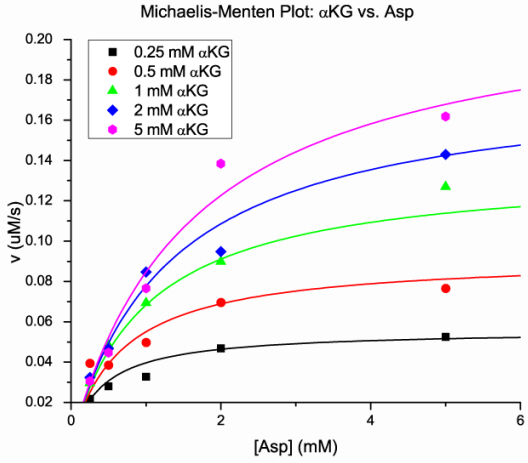

b. Grid #2

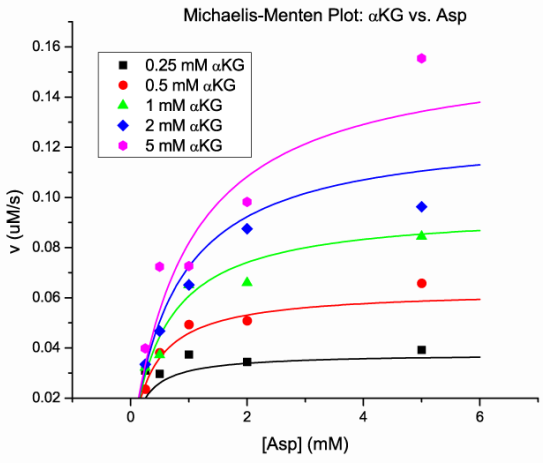

c. Grid #3

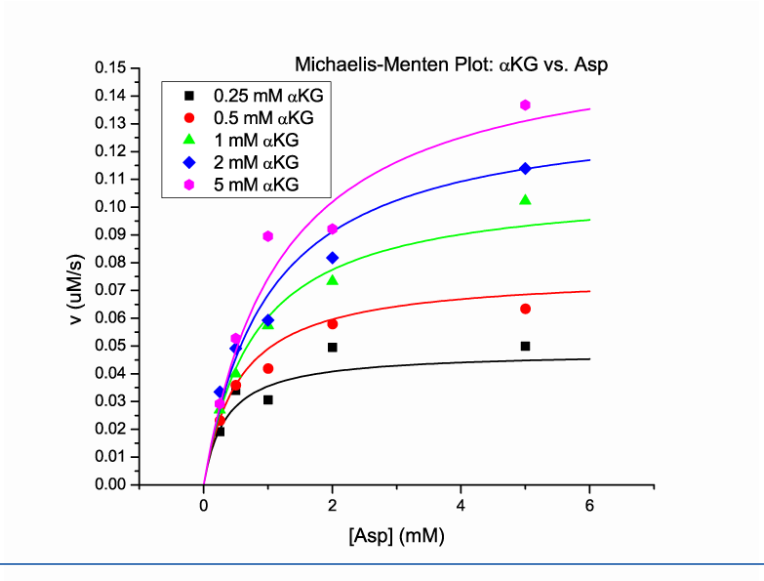

Figure 5. Lineweaver Burk Plots of 1/velocity vs. 1/[αKG], at varying concentrations of Asp

a. Grid #1

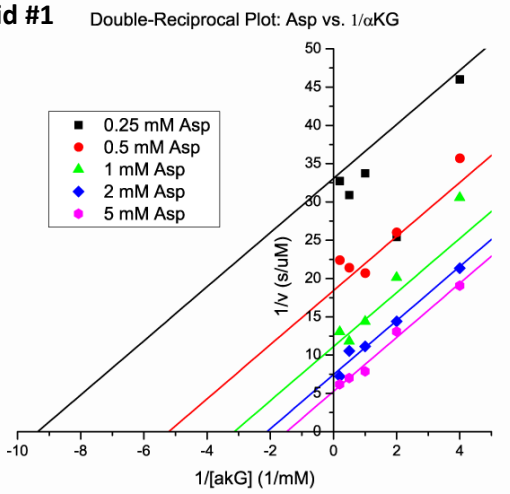

b. Grid #2

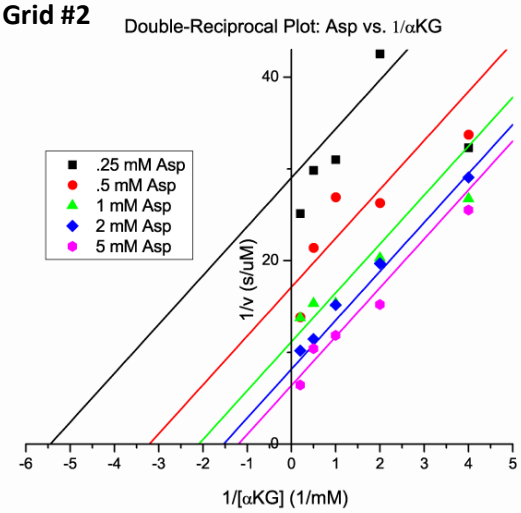

c. Grid #3

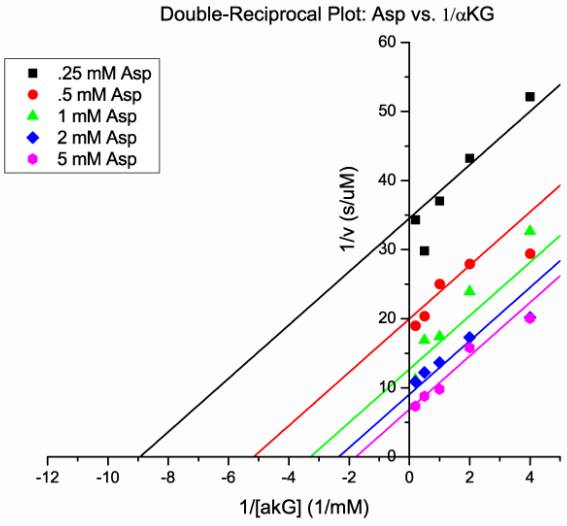

Figure 6. Lineweaver Burk Plots of 1/velocity vs. 1/[Asp], at varying concentrations of αKG

a. Grid #1

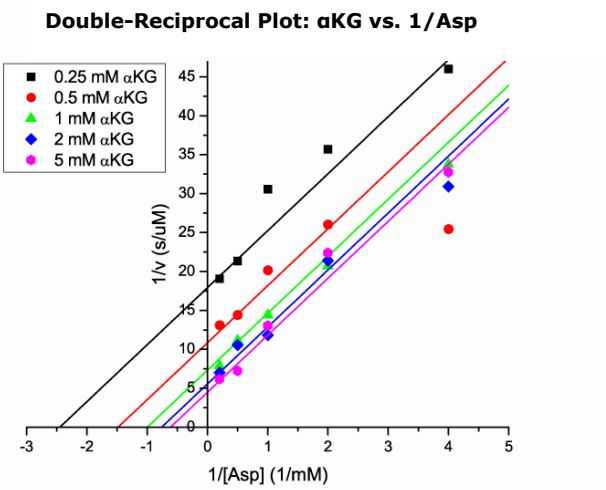

b. Grid #2

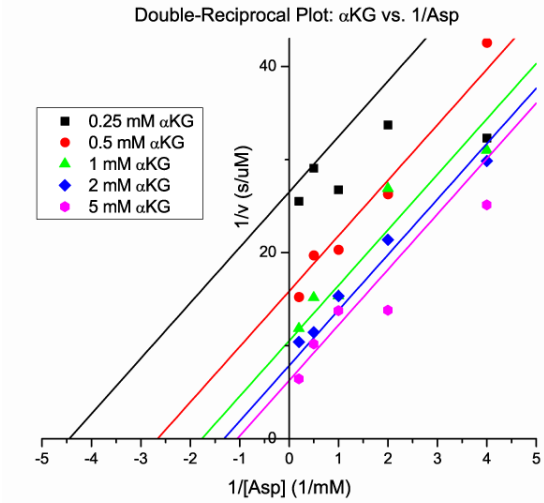

c. Grid #3

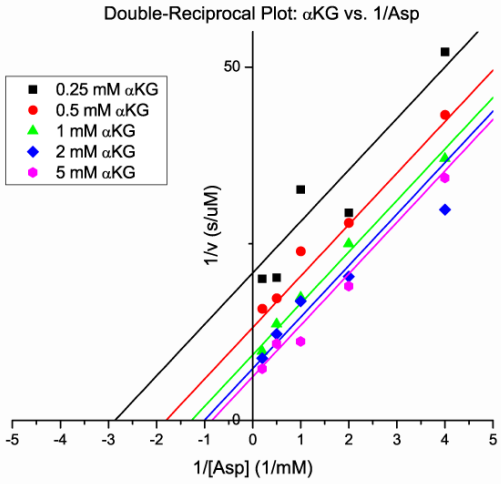

The nonlinear curve fitting of the data from Table 1 gave the K_m for each substrate and the V_{max} for each of the three kinetic assay grids. This kinetic data is collected in Table 2. Using this data, the weighted averages were calculated as seen in Table 3, with a K_m^{Asp} of 1.4 ± 0.1 mM, $K_m^{\alpha kG}$ of 0.71 ± 0.08 mM, a V_{max} of 0.205 ± 0.009 µM/s and k_{cat} of 149/s.

Table 2. Km, Vmax, and Standard Error from Curve Fitting

	K_m^{Asp}, mM	$K_m^{\alpha kG}$, mM	V_{max}, µM/s
Grid #1:	1.9 ± 0.2	0.9 ± 0.1	0.26 ± 0.02
Grid #2:	1.1 ± 0.2	1.0 ± 0.1	0.19 ± 0.02
Grid #3:	1.3 ± 0.1	0.7 ± 0.1	0.18 ± 0.01

Table 3. Average K_m, V_{max}, and k_{cat} from Data Grids 1-3

Weighted Averages and Error:	
K_m Asp:	1.4 ± 0.1 mM
K_m αKG:	0.71 ± 0.08 mM
V_{max}:	0.205 ±0.009 µM/s
k_{cat}:	149 ± 9/s

Steady State Kinetics of eAATase Using Phenylalanine. The data from k_{cat}/K_m determination is given in Table 4. The linear fit of each data set can be seen in Figure 7, the linear range of the Michaelis Menten plot, and the slope of these plots is V_{max}/K_m. From the slope of the linear fit of the data, the k_{cat}/K_m for phenylalanine is displayed in Table 5. Trials 2 and 3 were carried out together, and thus both data sets are combined for a linear fit, as seen in Figure 7b.

Table 4. Kinetic Assays Of Varying Concentrations of Phenylalanine

[Phe], mM	Reaction Rates, µM/s:		
	Trial 1	Trial 2	Trial 3
48	0.3766	0.4600	0.4642
24	0.2143	0.2148	0.2123
12	0.0863	0.0978	0.1104
6.0	0.0578	0.0556	0.0534
3.0	0.0250	0.0281	0.0287
1.5	0.0120	0.0167	0.0169
0.70	0.0051	0.0073	0.0067

Figure 7. Michaelis Menten Plots at low concentrations of phenylalanine

a. Trial 1

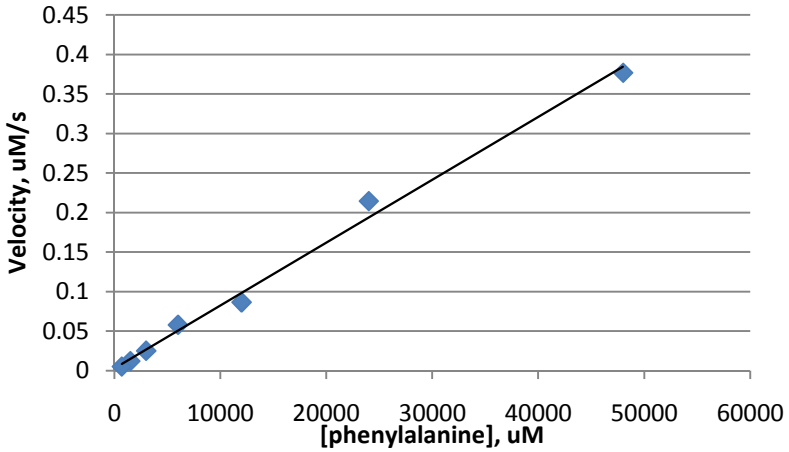

b. Trial 2 & 3[a]

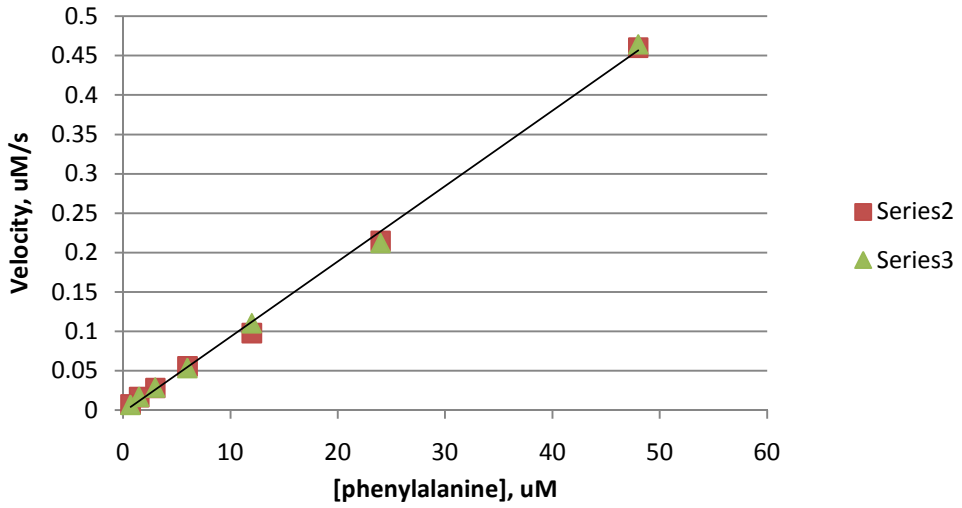

[a] Data from Trials 2 and 3, carried out simultaneously, were fit to a straight line, plotted here. Trial 2 data are represented as Series2 with red boxes. Trial 3 data are represented by Series3 with green triangles.

Table 5. k_{cat}/K_m for trials 1-3 and average k_{cat}/K_m

	Slope (V_{max}/K_m)		k_{cat}/K_m	
	Value (μs^{-1})	**Std. Error (μs^{-1})**	**Value ($M^{-1} s^{-1}$)**	**Error ($M^{-1} s^{-1}$)**
Trial #1:	7.95	0.255	115.62	0.0353
Trial #2:	9.50	0.214	138.14	0.0217
Trial #3:	9.57	0.183	139.03	0.0198
			Average:	**131 ± 9 $M^{-1} s^{-1}$**

DISCUSSION

The final k_{cat}/K_m values for both phenylalanine and aspartate are compiled in Table 6, including determinations in this research as well as values from previous publications. Additionally, a ratio of the k_{cat}/K_m^{Phe} to k_{cat}/K_m^{Asp} (Phe/Asp) was calculated to compare each enzyme's specificity for each substrate. It can be seen that the wild-type eAATase has a low specificity k_{cat}/K_m for phenylalanine as compared to aspartate, with a 1000-fold great specificity with aspartate for this research and previous research. In contrast, eTATase has a high specificity for both phenylalanine and aspartate.

Table 6: Comparison of final k_{cat}/K_m for Phe/Asp from current and previous research

	***Specificity:* K_{cat}/K_m ($\times 10^{-2} M^{-2} s^{-1}$)**		**Comparison of Specificity:**
enzyme	*Phe*	*Asp*	*Phe/Asp*
eAATase[a]	1.31	1010	0.0013
eAATase[b]	1.19 [c]	900 [d]	0.001
eTATase[e]	9600 [e]	370 [e]	26

[a] values determined from current study. [b] values determined in other publications. [c] from reference *17*. [d] from reference *7*. [e] values from reference *8*.

The kinetic assay method carried out for the eAATase reaction using aspartate as a substrate allowed for accurate baseline determinations of K_m values. As Table 3 indicates, the K_m for aspartate (1.4 ± 0.1 mM) and for α-ketoglutarate (0.71 ± 0.08 mM) both had error which included published K_m values: 1.3 mM and 0.77 mM respectively (18,19). The k_{cat} value determined for this reaction was 149 ± 9/s, which is within 2-fold of the published k_{cat} , a turnover number of 259/s. This 2-fold lower k_{cat} could be due to effects present in the kinetic assays affecting reaction rate, including viscosity or enzyme concentrations (20). Especially, different enzyme concentrations can account for the differences in turnover number, since k_{cat} is determined by the quotient of Vmax/[E]. Thus, it is important to note that numerous errors are present in the determination of enzyme concentration, including percent purity, making the k_{cat} determination prone to error.

Figures 3-6 show how well the data fit the simulation of the Michaelis Menten and Lineweaver Burk curves. Each of the three grids show well-fit data at lower concentrations of aspartate and α-ketoglutarate, however, at the higher concentrations the data shows more variation. At higher concentrations of substrate perhaps solution effects altered reaction rate such as viscosity, limiting the ability of the enzyme to turn over the substrates as quickly, lowering the k_{cat} as compared to previously published values (21).

k_{cat}/K_m values calculated in Table 6 were also found to correspond to published values of the wild-type eAATase. The calculated k_{cat}/K_m for aspartate (1.01×10^6 $M^{-1}s^{-1}$) and phenylalanine (131 $M^{-1}s^{-1}$) were similar to the published values of 119 $M^{-1}s^{-1}$ and 9.00×10^6 $M^{-1}s^{-1}$, respectively (7, 17). As expected, eAATase is a great catalyst for aspartate and a poor catalyst for phenylalanine, showing almost a 1000-fold higher specificity for aspartate than phenylalanine, with a ratio of k_{cat}/K_m^{Phe} to k_{cat}/K_m^{Asp} of 0.0013 (published ratio of 0.001 (2)). This is in contrast to eTATase, which has a published ratio of of k_{cat}/K_m^{Phe} to k_{cat}/K_m^{Asp} of 26 (8). The evaluation of the eAATase mutant specificity will be assessed by looking for an increase of the ratio of k_{cat}/K_m^{Phe} to k_{cat}/K_m^{Asp} towards that of eTATase.

Next in this research possible residues for mutagenesis is are being determined. As previous literature has shown, residue 39 is particularly involved in eAATase specificity so it will be mutated along with other residues predicted to affect the enzyme's specificity. The PyTrip computer program gives distances between residues from an input list of covarying residues. Potential candidate residue groups will be selected based on their proximity to the active site and distances between each other in the tertiary structure of the enzyme. Changes are currently being made to the PyTrip program to take into account that shorter distances may occur intermolecularly between homo dimers.

E. coli aspartate aminotransferase is the best understood of the PLP-dependent enzyme family. A vast amount of mechanistic, structural, and kinetic data is published for this enzyme, making it a model enzyme for the study of redesigning enzyme behavior (21). In the past, researchers have

successfully been able to change the specificity of aspartate aminotransferase using site-directed mutagenesis (11). Rational redesigning of enzymes uses structural and sequence alignment information to suggest possible effective substitutions, which are subsequently evaluated through site-directed mutagenesis and characterization of the expressed protein (11). In the current research, a specific computer program is used to look at covariation between unconserved residues, and these residues are evaluated for their role in the specificity of eAATase. If the resulting mutants show a change in eAATase specificity to that of eTATase, these current methods have many important applications in future research, medicine, and the pharmaceutical industry. Being able to use pattern changes of amino acid sequences to predict residues that will change enzyme behavior will be essential for furthering the field of enzyme engineering.

CONCLUSIONS

This current research established the kinetic baseline of the wild-type *E. coli* aspartate aminotransferase enzyme using aspartate and phenylalanine. Spectrophotometric determination of k_{cat}/K_m for both aspartate (1.01×10^6 $M^{-1}s^{-1}$) and phenylalanine (131 $M^{-1}s^{-1}$) served as the quantitative measure of the enzyme's current specificity. As expected, eAATase is a good catalyst for the transamination of aspartate, and a poor catalyst for phenylalanine giving a ratio of k_{cat}/K_m^{Phe} to k_{cat}/K_m^{Asp} of 0.0013 (published ratio of 0.001 (2)), as compared to eTATase which is an excellent catalyst for both substrates, and has a published ratio of 26 (8).This kinetic baseline is necessary in this project because it is required to assess the specificity of the mutant protein that will be expressed in the future. Currently, residues in eAATase predicted to change substrate specificity are being determined, then site-directed mutagenesis will be carried out and specificity characterization of the mutant will continue.

ACKNOWLEDGEMENTS

I thank Dr. Kathryn Muratore for the amazing opportunity to study in her lab, and her role as my capstone advisor, as well as the American University Chemistry Department for allowing me to conduct this capstone research project. I would also like to thank Donald Lee, Tim Borbet, Tamra Fisher, Jennifer Gaston, and Shannon Christie for their previous and current work on associated research. Especially, I would like to thank Sam Sheftel who has created the PyTrip program to allow choosing of residues for mutagenesis, and importantly Daniel Catt who, as part of an independent study, has carried out this research project with me.

REFERENCES

1. BRENDA: The Comprehensive Enzyme Information System. Schomburg, D. 18 Apr. 2011. <www.brenda-enzymes.org>.

2. Chow, MS, McElroy, KE, Corbett, KD, Berger, JM, and Kirsch, JF (2004). Narrowing Substrate Specificity in a Directly Evolved Enzyme: The A293D Mutant of Aspartate Aminotransferase. *Biochemistry*, *43*, 12780-1278.

3. John R.A. (1995). Pyridoxal phosphate-dependent enzymes. *Biochem Biophy Acta, 1248,* 81-96.

4. Malashkevich, V.N., Strokopytov, B.V., Zbigniew, D., Wilson, K.S., and Torchinsky, Y.M. (1995). Crystal Structure of the Closed Form of Chicken Cytosolic Aspartate Aminotransferase at 1.9 Å Resolution. *J. Mol. Biol., 247*, 111–124.

5. ChemAxon: Toolkits and Desktop Applications for Cheminformatics: Marvin. Grossman, R. B. 18 Apr. 2011. <http://www.chemaxon.com>.

6. Jager, J., Kohler, E., Tucker, P., Sauder, U., Housley-Markovic Z, Fotheringham I, Edwards M, Hunter M, Kirschner K, Jansonius JN (1989). Crystallization and preliminary X-ray studies of an aspartate aminotransferase mutant from Escherichia coli. J. Mol. Bio, 3, 499-501.

7. Gloss, L. M., and Kirsch, J. F. (1995) Decreasing the basicity of the active site base, Lys258, of *Escherichia coli* aspartate aminotransferase by replacement with gamma thialysine, *Biochemistry 34*, 3990−3998.

8. Hayashi, H., Inoue, K., Nagata, T., Kuramitsu, S. and Kagamiyama, H. (1993). *Escherichia coli* aromatic amino acid aminotransferase: characterization and comparison with aspartate aminotransferase. *Biochemistry.* 32, 12229−12239.

9. Jager, J., Pauptit, R. A., Sauder, U., and Jansonius, J. N. (1994) Three-dimensional structure of a mutant *E. coli* aspartate aminotransferase with increased enzymic activity, *Protein Eng. 7*, 605−612.

10. Onuffer, J. J., and Kirsch, J. F. (1995) Redesign of the substrate specificity of *Escherichia coli* aspartate aminotransferase to that of *Escherichia coli* tyrosine aminotransferase by homology modeling and site-directed mutagenesis, *Protein Sci. 4*, 1750−1757.

11. Rothman, S. C., Voorhies, M., and Kirsch, J. F. (2004) Directed evolution relieves product inhibition and confers *in vivo* function to a rationally designed tyrosine aminotransferase, *Protein Sci. 13*, 763−772.

12. Hayashi, H., Kuramitsu, S.M. and Kagamiyama, H. (1991). Replacement of an interdomain residue Val 39 of *Escherichia coli* aspartate aminotransferase affects the catalytic competence without altering the substrate specificity of the enzyme. *J. Biochem,* 109, 699−704.

13. Malashkevich, V. N., Onuffer, J. J., Kirsch, J. F., and Jansonius, J. N. (1995) Alternating arginine-modulated substrate specificity in an engineered tyrosine aminotransferase, *Nat. Struct. Biol. 2*, 548−553.

14. Dawson, R. Ben (1985). *Data for biochemical research*. Oxford: Clarendon Press, 122.

15. Copeland, R.A. (2000) in *Enzymes: A Practical Introduction to Structure, Mechanism, and Data Analysis,* primary pattern 355-357, Wiley-VCH, Toronto, Canada.

16. Jager, J., Moser, M., Sauder, U., and Jansonius, J. N. (1994) Crystal structures of *Escherichia coli* aspartate aminotransferase in two conformations. Comparison of an unliganded open and two liganded closed forms, *J. Mol. Biol. 239*, 285−305.

17. Luong, T. N., and Kirsch, J. F. (2001) A general method for the quantitative analysis of functional chimeras: Applications from site-directed mutagenesis and macromolecular association, *Protein Sci. 10*, 581−591.

18. Yagi T., Kagamiyama H., Nozaki M., Soda K. (1985). Glutamate-aspartate transaminase from microorganisms.*Methods Enzymol. 113,* 83-89.

19. Lo H.H., Hsu S.K., Lin W.D., Chan N.L., Hsu W.H. (2005). Asymmetrical synthesis of L-homophenylalanine using engineered Escherichia coli aspartate aminotransferase. *Biotechnol Prog. 21,* 411-415.

20. Deu E., Koch K.A., Kirsch J.F. (2002). The role of the conserved Lys68*:Glu265 intersubunit salt bridge in aspartate aminotransferase kinetics: multiple forced covariant amino acid substitutions in natural variants.*Protein Sci., 11,* 1062-1073.

21. Goldberg, J.M. and Kirsch, J.F. (1996). The Reaction Catalyzed by *Escherichia coli* Aspartate Aminotransferase Has Multiple Partially Rate-Determining Steps, While That Catalyzed by the Y225F Mutant Is Dominated by Ketimine Hydrolysis*. Biochemistry, 35,* 5280-5291.